Published in final edited form as:
Eur J Cardiothorac Surg. 2008 February ; 33(2): 191–197.

EFFECTS OF ACUTE ISCHEMIC MITRAL REGURGITATION ON THREE DIMENSIONAL MITRAL LEAFLET EDGE GEOMETRY

Wolfgang Bothe, MD[*], **Tom C. Nguyen, MD**[*], **Daniel B. Ennis, PhD**[*], **Akinobu Itoh, MD**[*], **Carl Johan Carlhäll, MD, PhD**[#,*], **David T. Lai, MD**[*], **Neil B. Ingels Jr., PhD**[#,*], and **D. Craig Miller, MD**[*]

[*]*Department of Cardiothoracic Surgery, Stanford University School of Medicine, Stanford, California*

[#]*Laboratory of Cardiovascular Physiology and Biophysics, Research Institute of the Palo Alto Medical Foundation, Palo Alto, California*

Abstract

Background: Improved quantitative understanding of *in-vivo* leaflet geometry in ischemic mitral regurgitation (IMR) is needed to improve reparative techniques, yet few data are available due to current imaging limitations. Using marker technology we tested the hypotheses that IMR: (1) Occurs chiefly during early-systole; (2) Affects primarily the valve region contiguous with the myocardial ischemic insult; and, (3) Results in systolic leaflet edge restriction.

Methods: Eleven sheep had radiopaque markers sutured as five opposing pairs along the anterior (A_1-E_1) and posterior (A_2-E_2) mitral leaflet free-edges from the anterior commissure (A_1-A_2) to the posterior commissure (E_1-E_2). Immediately postoperatively, biplane videofluoroscopy was used to obtain 4-D marker coordinates before and during acute proximal left circumflex artery occlusion. Regional mitral orifice area (MOA) was calculated in the anterior (Ant-MOA), middle (Mid-MOA) and posterior (Post-MOA) mitral orifice segments during early-systole (EarlyS), mid-systole (MidS), and end-systole (EndS). MOA was normalized to zero (minimum orifice opening) at baseline EndS. Tenting height was the distance of the midpoint of paired markers to the mitral annular plane at EndS. .

Results: Acute ischemia increased echocardiographic MR grade (0.5±0.3 vs. 2.3±0.7, $p<0.01$) and MOA in all regions at EarlyS, MidS and EndS: Ant-MOA (7±10 vs. 22±19mm^2, 1±2 vs. 18 ±16mm^2, 0 vs. 17±15mm^2); Mid-MOA (9±13 vs. 25±17mm^2, 3±6 vs. 21±19mm^2, 0 vs. 25 ±17mm^2); and Post-MOA (8±10 vs. 25±16, 2±4 vs. 22±13mm^2, 0 vs. 23±13mm^2), all $p<0.05$. There was no change in MOA throughout systole (EarlyS vs. MidS vs. EndS) during baseline conditions or ischemia. Tenting height increased with ischemia near the central and the anterior commissure leaflet edges (B_1-B_2: 7.1±1.8mm vs. 7.9±1.7mm, C_1-C_2: 6.9±1.3mm vs. 8.0±1.5mm, both $p<0.05$).

Conclusions: (1) MOA during ischemia was larger throughout systole, indicating that acute IMR in this setting is a holosystolic phenomenon; (2) Despite discrete posterolateral myocardial ischemia, Post-MOA was not disproportionately larger; (3) Acute ovine IMR was associated with leaflet restriction near the central and the anterior commissure leaflet edges. This entire constellation of annular, valvular, and subvalvular ischemic alterations should be considered in the approach to mitral repair for IMR.

Address for correspondence: D. Craig Miller, M.D. Department of Cardiothoracic Surgery Falk Cardiovascular Research Center Stanford University School of Medicine Stanford, California 94305-5247 001.650.725.3826 FAX 001.650.725.3846 E-mail: dcm@stanford.edu.

Presented in part at the 21st Annual Meeting of the European Society of Cardiothoracic Surgery, Geneva, September 2007

Keywords

acute myocardial ischemia; ischemic mitral regurgitation; mitral orifice area; radiopaque markers; ovine model

INTRODUCTION

Ischemic mitral regurgitation (IMR) is associated with alterations in mitral leaflet geometry resulting from annular and subvalvular left ventricular (LV) remodeling [1-4]. Improved understanding of leaflet geometry during IMR is needed to refine techniques for mitral valve (MV) repair. Due to limitations inherent in standard imaging techniques, however, there are little four-dimensional (4D) quantitative data describing regional MV geometry. MRI and ultrasound either lack sufficient temporal resolution and/or the ability to track accurately specific anatomical fiduciary loci on the leaflets throughout the cardiac cycle. This may, in part, explain existing controversies about IMR such as the question: "When in the cardiac cycle is regurgitation present?" [5-8]. While heart murmurs due to IMR are heard mostly during late systole [5], leaflet malcoaptation during IMR has been described as a "biphasic" (throughout systole with peaks during early and late systole) [6,7] or early systolic [8] phenomenon.

Controversy also exists regarding which region of the mitral valve is affected most by ischemia. While some studies suggest the valve region adjacent to the ischemic insult is predominantly involved [9] spawning the development of asymmetrical annuloplasty rings [10], other studies suggest that ischemia may affect the mitral valve uniformly [11].

In this ovine study, we used radiopaque leaflet markers and 4-D tracking to quantify the precise temporal and regional changes in mitral leaflet edge geometry along the entire coaptation line before and during acute IMR. We tested the hypotheses that IMR: (1) Occurs chiefly during early-systole; (2) Affects primarily the valve region adjacent to the ischemic insult; and, (3) Results in systolic leaflet edge restriction.

MATERIALS AND METHODS

All animals received humane care in compliance with the Principles of Laboratory Animal Care formulated by the National Society for Medical Research and the Guide for Care and Use of Laboratory Animals prepared by the National Academy of Sciences and published by the National Institutes of Health (DHEW [NIH] Publication 85 to 23, revised 1985). This study was approved by the Stanford Medical Center Laboratory Research Animal Review Committee and conducted according to Stanford University policy.

Surgical Preparation

Miniature radiopaque markers were surgically implanted in 11 adult castrated male sheep (73 ±8 kg). Other calculations using the similar datasets have been published previously and technical details will therefore only be summarized briefly [12]. Ten markers were sutured as opposing pairs along the anterior and posterior mitral leaflet free-edges (Fig 1A). Five radiopaque markers (A_1-E_1) were placed on the anterior mitral leaflet (AML) edge from the anterior commissure (ACOM; #16) to the posterior commissure (PCOM; #20), with marker C_1 at central leaflet edge. Five corresponding markers (A_2-E_2) were placed on the posterior mitral leaflet (PML) edge. Eight markers were sutured equidistantly around the mitral annulus. Additional markers were placed on the tips of the anterior and posterior papillary muscles (PM).

Experimental Protocol

Postoperatively, animals were transferred under acute open chest conditions to the experimental catheterization laboratory and studied intubated and anesthetized with inhalational isoflurane (1.5–2.0%). Simultaneous biplane videofluoroscopic and hemodynamic data were acquired before and during acute posterolateral LV ischemia (2 - 3 minute occlusion of left circumflex artery proximal to the first obtuse marginal artery) and IMR was assessed via transesophageal echocardiography. Mitral regurgitation was graded semi-quantitatively based on Doppler regurgitant jet extent and width as none (0), trace (+0.5), mild (+1), moderate (+2), moderate-severe (+3), or severe (+4) from a 3-chamber view. Before and following ischemia, biplane videofluoroscopic images were acquired at 60Hz, digitized, and merged to yield 3-D coordinates every 16.7 ms using custom designed software [13,14]. Simultaneous analog LV pressure and electrocardiographic voltage were digitized and recorded on the images.

Data Analysis

Data from 3 consecutive hemodynamically stable beats during control and acute ischemic conditions were averaged and analyzed. Figure 2 illustrates the time points used. ED was defined as the frame nearest the R-wave on the ECG. EndS was defined as the frame immediately preceding the peak negative rate of LV pressure change (−dP/dtmax). EarlyS was defined as within 102ms (six frames) after end diastole (representing the early phase of ejection) and MidS as the time-point between end diastole (ED) and EndS.

Total mitral orifice area

To determine the timing and duration of IMR during acute ischemia, total mitral orifice area (MOA) was defined as the sum of areas between all triplets of commissural and leaflet markers (Fig 1B) at EarlyS, MidS and EndS before and during ischemia. To facilitate data comparison between hearts with variable marker locations the MOA at baseline at EndS (when there should be complete coaptation and minimum orifice opening) was calculated for each heart and subtracted from all other MOA values for that heart. Raw values were used for all statistical analyses.

Regional mitral orifice area

To understand the effect of ischemia on different regions of the mitral valve, the MOA was subdivided into anterior (Ant-MOA), middle (Mid-MOA) and posterior (Post-MOA) segments (Fig 1B). Regional MOA's were calculated as the sum of areas of the following triangles: Ant-MOA (#16-A_1-A_2 + A_1-A_2-B_2 + A_1-B_2-B_1); Mid-MOA (B_1-B_2-C_2 + B_1-C_2-C_1 + C_1-C_2-D_1 + C_2-D_1-D_2); and Post-MOA (D_1-D_2-E_1 + D_2-E_1-E_2 + E_1-E_2-#20), Figure 1B.

Tenting geometry

To assess leaflet edge restriction due to PM tethering, tenting height along the mitral coaptation line was obtained by calculating the distance from the midpoint of each of the paired markers (A_1-A_2, B_1-B_2, C_1-C_2, D_1-D_2, E_1-E_2) to the best-fit plane of all annular markers at EndS during control and ischemia as described earlier [4]. To gain insight into regional changes of the respective mitral leaflet edges during acute ischemia, distances of each AML and PML edge marker to the annular plane at EndS were calculated.

Mitral annular dimensions

For each frame, annular diameters were calculated as distances between the respective annular markers. To evaluate ischemia-related regional mitral annular changes, mitral annular septal-lateral diameters were determined for the anterior (S-L_{ANT}=distance between markers #15 and

#17), middle (S-L_{MID}=distance between markers #22 and #18 and posterior (S-L_{POST}=distance between markers #21 and #19) annular regions. The commissure-commissure (C-C) annular dimension was defined as the distance between the markers #16 and #20. Mitral annular area (MAA) was computed as the sum of 8 triangular areas formed by consecutive adjacent marker pairs along the annulus and the annular centroid as previously described [15].

Tethering lengths

Tethering lengths were calculated as proposed by Messas *et al.* [16] as the distance of anterior and posterior PM tips to the annular saddle-horn marker (#22, Fig 1A.).

Statistical Analysis

All results are reported as mean ±1SD unless otherwise stated. The geometric variables measured before and during ischemia were compared using a two-tailed Student's t-test for paired observations. For comparisons between different time points, a one-way ANOVA for repeated measurements with a Holm-Sidak post-hoc test was performed (Sigmastat 2.03, SPSS, Chicago, IL). $P<0.05$ was considered statistically significant.

RESULTS

Hemodynamics

Table 1 summarizes the hemodynamic data. MR grade was 0.5±0.3 before and 2.3±0.7 ($p<0.01$) during ischemia. Maximum LV dP/dt decreased (1,950±600 vs. 1,120±290 mmHg/s, $p<0.01$) while LVEDP increased with acute ischemia (18±3 vs. 25±5 mmHg, $p<0.01$), indicating impaired LV filling. Systolic LV pressure fell as ejection progressed during both baseline and ischemic conditions (EarlyS vs. EndS and midS vs. EndS, $p<0.01$).

Total mitral orifice area

Figure 3 shows normalized total MOA throughout systole (EarlyS, MidS, and EndS). As noted above, the data were normalized to baseline EndS assuming minimum orifice opening at that time point. Total MOA was larger during ischemia throughout systole (EarlyS: 24.4±9.5 vs. 71.7±12.7, MidS: 6.4±3.0 vs. 60.8±11.9 and EndS: 0 vs. 65.0±11.2, all $p<0.01$). At baseline and during ischemia, total MOA did not change during systole (EarlyS vs. MidS vs. EndS, all N.S.).

Regional mitral orifice area

Figure 4 shows the normalized MOA calculated for the different coaptation regions during earlyS, midS and EndS. Ischemia increased MOA in all three regions at EarlyS, MidS and EndS (all $p<0.05$): Ant-MOA (7±10 vs. 22±19mm^2, 1±2 vs. 18±16mm^2, 0 vs. 17±15mm^2); Mid-MOA (9±13 vs. 25±17mm^2, 3±6 vs. 21±19mm^2, 0 vs. 25±17mm^2); and Post-MOA (8±10 vs. 25±16, 2±4 vs. 22±13mm^2, 0 vs. 23±13mm^2). Similar to total MOA, regional MOA did not change during systole during both baseline and ischemic conditions (EarlyS vs. MidS vs. EndS, all N.S.).

Tenting geometry

Figure 5A shows the tenting height along the mitral coaptation line before and during ischemia. Tenting height increased with ischemia in the regions near the anterior commissure and central leaflet edge (marker pairs B1-B2 and C1-C2) but not in the region of the ischemic insult. With the exception of the posterior commissure region (marker D1, Fig 5B), the distance from the AML edge markers to the annular plane did not change with ischemia. Marker D1 moved toward the mitral annular plane (prolapse direction) with ischemia despite the outward

displacement of the posterior PM (Table 3). Ischemic alterations of the PML-edge were more complex (Fig 5C): Marker E2 (PCOM) moved towards the mitral annular plane (prolapse) with ischemia whereas markers and C2 on the anterior and central edge of the PML moved away from the mitral annular plane, indicating leaflet restriction.

Mitral annular dimensions

Mitral annular dimensions are shown in Table 2. MAA as well as annular S-L and C-C diameters increased significantly with ischemia during all time points assessed. Ischemia increased annular S-L diameters in all three regions ($S\text{-}L_{ANT}$ vs. $S\text{-}L_{MID}$ vs. $S\text{-}L_{POST}$) throughout systole reflecting a homogeneous increase in mitral annular septal-lateral dimensions.

Tethering lengths

Tethering lengths during systole are shown in Table 3. Although the distance of the posterior PM-tip to the saddle-horn marker (#22) was greater with ischemia at any time point assessed, this greater distance reached statistical significance only for midS ($p<0.05$) and endS ($p<0.01$). As expected, the tip of the anterior PM did not displace significantly during postero-lateral ischemia.

DISCUSSION

This ovine study was designed to gain detailed insight into geometrical changes of both the anterior and posterior mitral leaflet edges along the entire coaptation line during acute IMR. The key (and surprising) findings of this study were that posterolateral LV ischemia produced: (1) A holosystolic increase of MOA; (2) A homogeneous increase of MOA in all three regions; and, (3) PML restriction near the anterior commissure and the central leaflet edge simultaneous with slight type II (prolapse) motion of both leaflets near the posterior commissure.

Hemodynamics

As stated by Levine and Schwammenthal, the equilibrium position of the mitral leaflets is determined by the balance of forces acting on them, including annular and PM tethering forces and closing forces generated by the ventricle [5]. It has been suggested that once tethering is increased, leaflet closure is further impaired when less force (*i.e.*, lower LV pressure) is available to oppose tethering. Schwammenthal *et al.* recognized a biphasic pattern of regurgitant orifice area in patients with chronic IMR with peaks in early and late systole and a decrease during mid systole [6] using echocardiography. They ascribed their findings to a mid systolic peak in LV pressures maximizing leaflet closing force. In our acute study, however, MOA remained constant throughout systole despite significantly lower LV pressures. These findings therefore suggest that the distortions in leaflet geometry induced by posterior PM tethering are not affected by alterations in LV-generated closing forces.

Total mitral orifice area

Controversy exists surrounding timing and duration of IMR with descriptions ranging from an early or late systolic [8] to a “biphasic” event [6]. The ischemia related increase in total MOA throughout systole found in this acute ovine experiment suggests that IMR in this setting is a *holosystolic* phenomenon. This finding is in contrast to earlier studies from our laboratory, which suggested a delayed closing motion of the mitral leaflets (early systolic mitral leaflet “loitering”) as a mechanism causing acute IMR [8]; however, in these previous experiments, a smaller ischemic insult was induced (occlusion of the mid-LCx artery), which did not result in posterior PM displacement. In the current ovine study, tethering length of the posterior PM significantly increased at MidS and EndS suggesting that tethering effects via the posterior PM

present predominantly during the middle and late phase of ventricular ejection. It may therefore be reasonable to speculate that the occurrence of local PM tethering during MidS and EndS contributed to "sustained" IMR throughout systole.

Regional mitral orifice area

In contrast to previous reports [9], separation of total MOA into regional segments (ANT, MID, POST) revealed that the increase in total MOA was not confined just to the region adjacent to the ischemic insult. A possible explanation for this may be that although the PM's were regionally affected (Tab 3) annular dilatation was not confined just to the posterolateral annular circumference, but was more global around the entire annulus (Tab 2). This, in turn, may have affected all regions of the coaptation line in a uniform manner.

Tenting geometry

Mitral valve tenting height reflected leaflet restriction during IMR in the regions near the central leaflet edge and the anterior commissure. To separate the effects of geometrical changes of AML and PML edges on tenting height calculations, distances of AML- and PML-edge markers to the annular plane were assessed, revealing that both AML and PML edges prolapsed in the region near the posterior commissure during acute ischemia despite an increase in tethering length of the posterior PM. Furthermore, the PML edge was restricted both near the anterior commissure and the central leaflet edge. These observations indicate that (1) a homogeneous increase in MOA is not necessarily associated with uniform changes in leaflet tenting geometry; (2) Changes in tenting height during IMR were mostly due to alterations in PML edge geometry; and (3) An increase in tethering length of the posterior PM during acute IMR may not only be associated with leaflet edge restriction but also with leaflet edge prolapse.

Two different explanations may account for this composite finding of local tethering via the posterior PM together with leaflet prolapse in the adjacent coaptation region. First, the chordae tendineae may originate from different heads of the PM which may be affected differently by the ischemic insult: Some PM heads may suffer ischemic dysfunction while others may still contract normally resulting in either too short, normal or too long a tethering length. We cannot draw any concrete conclusions here because only one PM tip had markers placed. Second, the direction of posterior PM displacement (apical, posterior, lateral, *etc*.) may affect leaflet edge geometry along the coaptation line differently. Imagine the mitral leaflet as a kite attached to the PM's via multiple strings (chordae), PM dislocation may put tension on some and slack on others strings resulting in either leaflet restriction or prolapse. If this is the case, the direction of PM-dislocation in 3-D space may therefore be important regarding our strategies to restore subvalvular LV geometry during mitral valve repair. This notion is supported by the work of Langer *et al*. in this laboratory who observed that pulling the head of the posterior PM in different directions attenuates MR differently in sheep with acute IMR[17]. Further work is needed to delineate which of these two, or perhaps a combination of both, is the main underlying mechanism.

Clinical Inferences

If mechanisms of IMR in patients follow a similar fashion, our observations may have implications for treating IMR. Regarding the homogeneous increase in regional MOA and regional S-L diameters, reparative surgical devices and interventional catheter approaches which modify all regions of the mitral annulus might confer superior durability. Regarding the complex alterations in leaflet tenting geometry, these data argue for the need to address both annular and subvalvular (LV) abnormalities; furthermore, a more sophisticated restoration of the subvalvular geometry may improve treatment results. A better understanding and more detailed preoperative evaluation of the subvalvular apparatus (including measuring tethering lengths of different PM heads and a determination of the PM tip displacement in 3-D space)

together with knowing 3-D leaflet tenting geometry along the coaptation line may allow more complete valve repair. Improvement in clinical imaging modalities beyond those currently available will help to measure these parameters.

Study Limitations

This investigation of acute IMR in an open-chest ovine model with previously healthy animals is quite different from the clinical scenario of patients with chronic IMR. Caution should therefore be exercised in extrapolating our findings to patients with chronic ischemic MR. Previous studies performed in our lab have shown that displacement of the PMs differs slightly in acute compared to chronic ischemia: In an ovine model of acute IMR Lai *et al*. [18] found antero-apical and postero-basal displacement of the anterior and posterior PM tips, respectively. Tibayan *et al.* [19] induced chronic IMR in sheep and noted postero-lateral and postero-lateral plus basal displacement of the anterior and posterior PM tips, respectively. Presumably such differences in 3-D PM behavior between acute and chronic ischemia will affect 3-D leaflet edge geometry; however, in clinical practice chronic ischemia and infarction resulting in IMR is not a single entity but instead is a constellation of different perturbations of the left ventricle with a common downstream result, MR. Thus, understanding the complete pattern of all regional LV wall thickening and motion abnormalities should increase our understanding of how the ventricle, subvalvular structures, and mitral leaflets interact.

Anatomical differences between ovine and human hearts, such as the more heavily scalloped posterior leaflet in sheep and different anatomical position of the PM's, means caution should be exercised when extrapolating the results of animal studies to humans.

Although markers were placed as close to the leaflet edges as possible, they may actually not have been within the coaptation line or region itself. Finally, no ventricular markers were placed, which precluded the analysis of LV shape or preload in this experiment.

Conclusions

In our ovine study acute discrete posterolateral myocardial ischemia resulted in an increase of MOA throughout systole, showing that acute IMR is a holosystolic phenomenon in this experimental model. The increase observed occurred uniformly across all regions of the mitral leaflet edges demonstrating that IMR was not predominantly confined to the valve region adjacent to the ischemic insult. Furthermore, acute IMR was associated with PML restriction near the anterior commissure and the central leaflet edge simultaneously along with prolapse of both leaflets near the posterior commissure. This complex pattern of leaflet geometric perturbations reflects the sum of annular and subvalvular alterations associated with LV ischemia that needs to be appreciated in the development of newer techniques and devices for valve repair in patients with IMR.

ACKNOWLEDGEMENTS

The authors gratefully acknowledge the expert technical assistance of Carol W. Mead, B.A and the thoughtful comments of Julia Swanson, M.D..

Supported by grants HL-29589 and HL-67025 from the National Heart, Lung and Blood Institute. Dr. Bothe was supported by the Deutsche Herzstiftung, Frankfurt, Germany. Dr. Carlhäll was supported by the Swedish Heart and Lung Foundation and the County Council of Östergötland, Sweden. Drs. Nguyen and Lai were Leah McConnell Cardiovascular Surgical Research Fellows. Dr. Nguyen was recipient of the Thoracic Surgery Foundation Research Fellowship. Dr. Ennis is supported by NHLBI Pathway to Independence K99-R00 HL-087614. Dr. Lai was supported by a fellowship from the American Heart Association, Western States Affiliate

REFERENCES

1. Gorman JH 3rd, Gorman RC, Jackson BM, Enomoto Y, John-Sutton MG, Edmunds LH Jr. Annuloplasty ring selection for chronic ischemic mitral regurgitation: lessons from the ovine model. Ann Thorac Surg 2003;76(5):1556–63. [PubMed: 14602285]
2. Watanabe N, Ogasawara Y, Yamaura Y, Wada N, Kawamoto T, Toyota E, Akasaka T, Yoshida K. Mitral annulus flattens in ischemic mitral regurgitation: geometric differences between inferior and anterior myocardial infarction: a real-time 3-dimensional echocardiographic study. Circulation 2005;112(9 Suppl):I458–62. [PubMed: 16159863]
3. Kumanohoso T, Otsuji Y, Yoshifuku S, Matsukida K, Koriyama C, Kisanuki A, Minagoe S, Levine RA, Tei C. Mechanism of higher incidence of ischemic mitral regurgitation in patients with inferior myocardial infarction: quantitative analysis of left ventricular and mitral valve geometry in 103 patients with prior myocardial infarction. J Thorac Cardiovasc Surg 2003;125(1):135–43. [PubMed: 12538997]
4. Tibayan FA, Wilson A, Lai DT, Timek TA, Dagum P, Rodriguez F, Zasio MK, Liang D, Daughters GT, Ingels NB Jr. Miller DC. Tenting volume: three-dimensional assessment of geometric perturbations in functional mitral regurgitation and implications for surgical repair. J Heart Valve Dis 2007;16(1):1–7. [PubMed: 17315376]
5. Levine RA, Schwammenthal E. Ischemic mitral regurgitation on the threshold of a solution: from paradoxes to unifying concepts. Circulation 2005;112(5):745–58. [PubMed: 16061756]
6. Schwammenthal E, Popescu AC, Popescu BA, Freimark D, Hod H, Eldar M, Feinberg MS. Mechanism of mitral regurgitation in inferior wall acute myocardial infarction. Am J Cardiol 2002;90(3):306–9. [PubMed: 12127618]
7. He S, Fontaine AA, Schwammenthal E, Yoganathan AP, Levine RA. Integrated mechanism for functional mitral regurgitation: leaflet restriction versus coapting force: in vitro studies. Circulation 1997;96(6):1826–34. [PubMed: 9323068]
8. Glasson JR, Komeda M, Daughters GT, Bolger AF, Karlsson MO, Foppiano LE, Hayase M, Oesterle SN, Ingels NB Jr. Miller DC. Early systolic mitral leaflet “loitering” during acute ischemic mitral regurgitation. J Thorac Cardiovasc Surg 1998;116(2):193–205. [PubMed: 9699570]
9. Dayan JH, Oliker A, Sharony R, Baumann FG, Galloway A, Colvin SB, Miller DC, Grossi EA. Computer-generated three-dimensional animation of the mitral valve. J Thorac Cardiovasc Surg 2004;127(3):763–9. [PubMed: 15001905]
10. Daimon M, Fukuda S, Adams DH, McCarthy PM, Gillinov AM, Carpentier A, Filsoufi F, Abascal VM, Rigolin VH, Salzberg S, Huskin A, Langenfeld M, Shiota T. Mitral valve repair with Carpentier-McCarthy-Adams IMR ETlogix annuloplasty ring for ischemic mitral regurgitation: early echocardiographic results from a multi-center study. Circulation 2006;114(1 Suppl):I588–93. [PubMed: 16820643]
11. Agricola E, Oppizzi M, Maisano F, De Bonis M, Schinkel AF, Torracca L, Margonato A, Melisurgo G, Alfieri O. Echocardiographic classification of chronic ischemic mitral regurgitation caused by restricted motion according to tethering pattern. Eur J Echocardiogr 2004;5(5):326–34. [PubMed: 15341868]
12. Lai DT, Tibayan FA, Myrmel T, Timek TA, Dagum P, Daughters GT, Liang D, Ingels NB Jr. Miller DC. Mechanistic insights into posterior mitral leaflet inter-scallop malcoaptation during acute ischemic mitral regurgitation. Circulation 2002;106(12 Suppl 1):I40–I45. [PubMed: 12354707]
13. Niczyporuk MA, Miller DC. Automatic tracking and digitization of multiple radiopaque myocardial markers. Comput Biomed Res 1991;24(2):129–42. [PubMed: 2036779]
14. Daughters G, Sanders W, Miller D, Schwarzkopf A, Mead C, Ingels N. A comparison of two analytical systems for 3-D reconstruction from biplane videoradiograms. IEEE Computers in Cardiology 1989;15:79–82.
15. Langer F, Rodriguez F, Cheng A, Ortiz S, Nguyen TC, Zasio MK, Liang D, Daughters GT, Ingels NB, Miller DC. Posterior mitral leaflet extension: an adjunctive repair option for ischemic mitral regurgitation? J Thorac Cardiovasc Surg 2006;131(4):868–77. [PubMed: 16580446]
16. Messas E, Guerrero JL, Handschumacher MD, Chow CM, Sullivan S, Schwammenthal E, Levine RA. Paradoxic decrease in ischemic mitral regurgitation with papillary muscle dysfunction: insights

from three-dimensional and contrast echocardiography with strain rate measurement. Circulation 2001;104(16):1952–7. [PubMed: 11602500]

17. Langer F, Rodriguez F, Ortiz S, Cheng A, Nguyen TC, Zasio MK, Liang D, Daughters GT, Ingels NB, Miller DC. Subvalvular repair: the key to repairing ischemic mitral regurgitation? Circulation 2005;112(9 Suppl):I383–9. [PubMed: 16159851]
18. Lai DT, Timek TA, Tibayan FA, Green GR, Daughters GT, Liang D, Ingels NB Jr. Miller DC. The effects of mitral annuloplasty rings on mitral valve complex 3-D geometry during acute left ventricular ischemia. Eur J Cardiothorac Surg 2002;22(5):808–16. [PubMed: 12414050]
19. Tibayan FA, Rodriguez F, Zasio MK, Bailey L, Liang D, Daughters GT, Langer F, Ingels NB Jr. Miller DC. Geometric distortions of the mitral valvular-ventricular complex in chronic ischemic mitral regurgitation. Circulation 2003;108(Suppl 1):II116–21. [PubMed: 12970219]

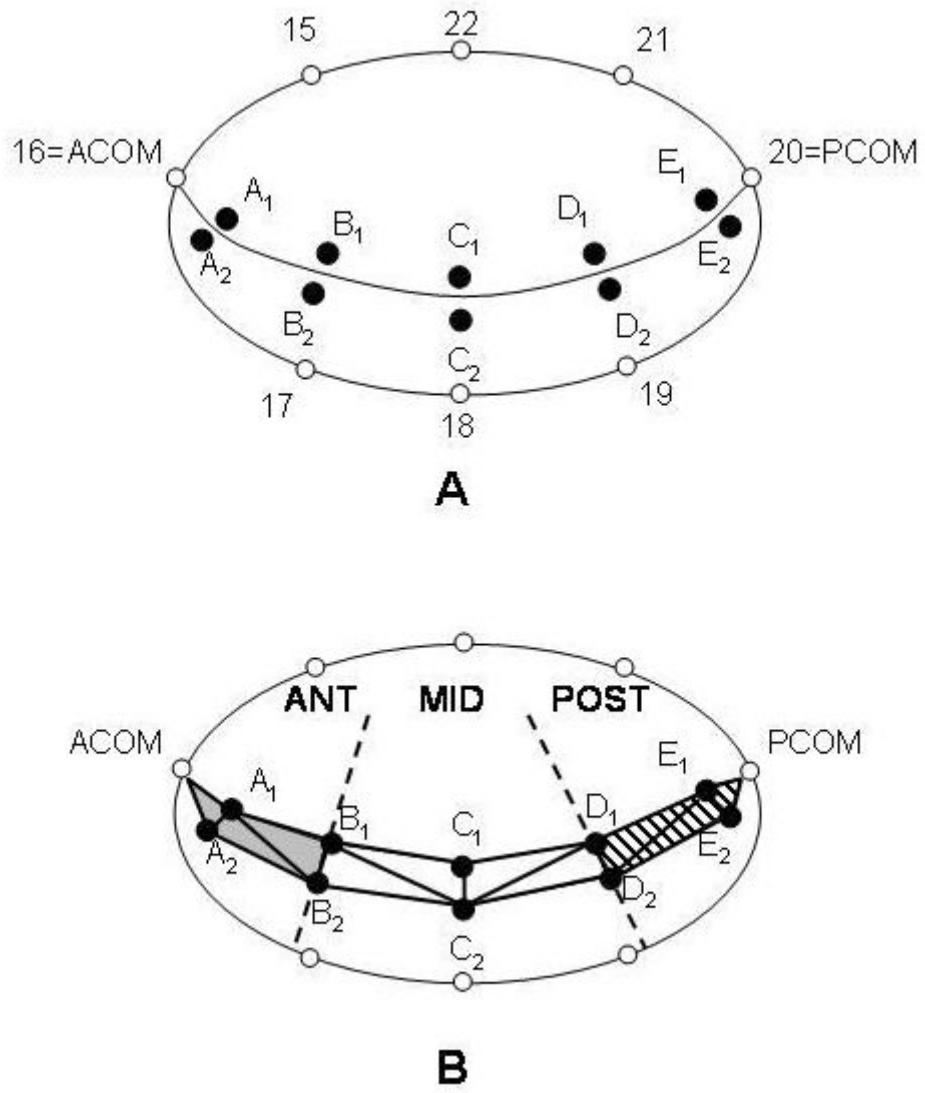

Fig 1.

A: Marker array used in this study. Ten radiopaque markers were sutured as opposing pairs along the anterior and posterior mitral leaflet free-edges. Five markers (A_1-E_1) were placed on the anterior mitral leaflet (AML) edge from the anterior commissure (ACOM; marker 16) to the posterior commissure (PCOM; marker 20), with marker C1 at central leaflet edge; five markers (A_2-E_2) were placed on the opposing PML; and eight markers were sewn on the annulus. **B**: Calculation of regional mitral orifice area (MOA): regional MOA was calculated as the sum of areas between triplets of commissural and leaflet markers in anterior (ANT, grey), middle (MID, white) and posterior (POST, checkered) mitral orifice segments, see METHODS for detailed description.

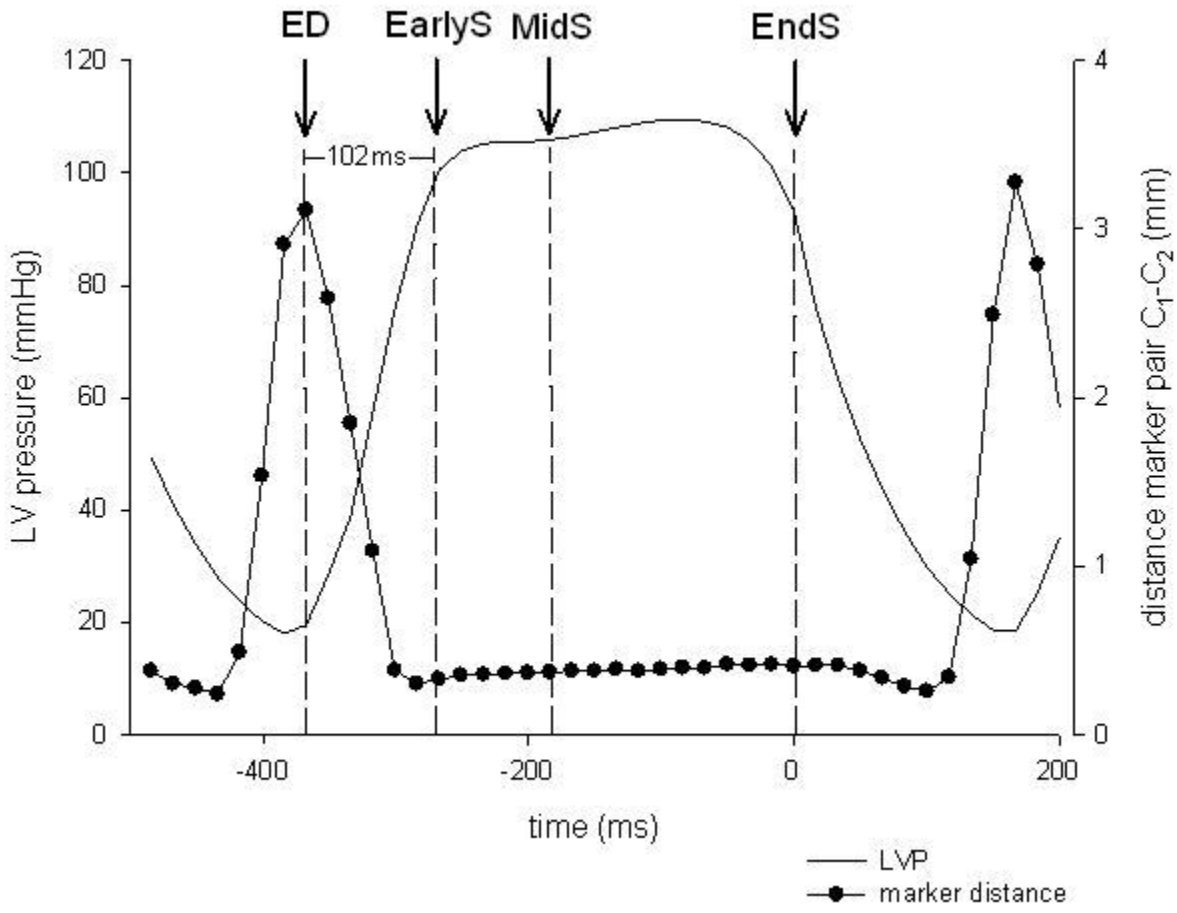

Fig 2.

Schematic to illustrate the determination of time points used. The black line shows LVP and the closed circles represent the plotted distances between the mid-edge marker pair C_1-C_2 from one representative study under baseline conditions. Greatest separation occurred during early filling and minimal separation occurred during systole during baseline conditions. Mitral orifice area was quantified during the early, mid-, and end-systolic phases. EndS was defined as the frame immediately preceding the peak negative rate of LV pressure change (-dP/dtmax), EarlyS was defined as within 102ms (six frames) after end diastole (representing the early phase of ejection) and MidS as the time-point between end diastole (ED) and EndS. ED was defined as the frame nearest the R-wave on the ECG.

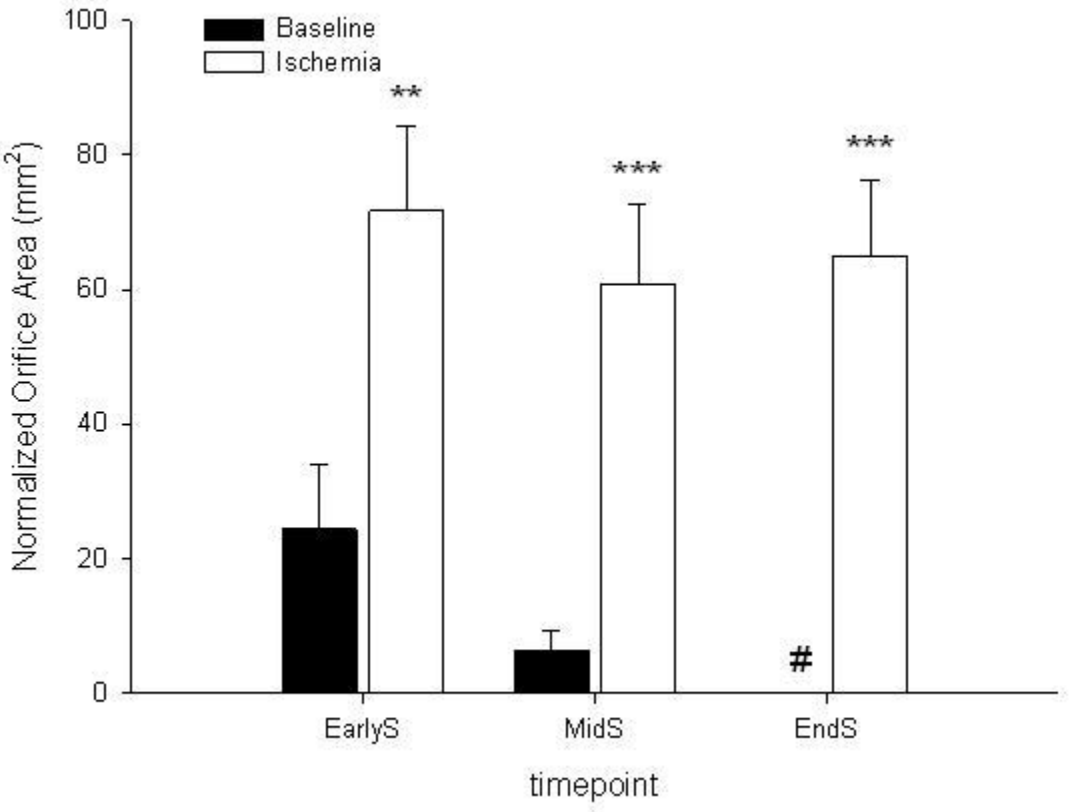

Fig 3.

Normalized total orifice area at early systole (earlyS);, mid-systole (midS) and end-systole (endS), # = to facilitate data comparison data was zeroed at baseline EndS assuming minimum orifice opening under baseline conditions at that timepoint (see METHODS for details), *=p<0.05 vs baseline, **=p<0.01 vs baseline, ***=p<0.001 vs baseline, data are group mean ±SEM

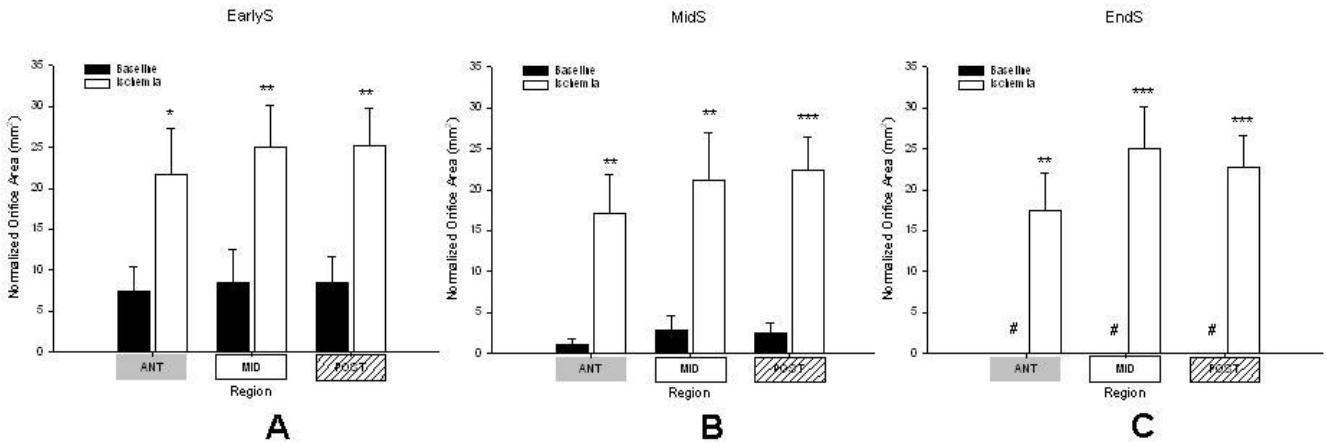

Fig 4.

Normalized regional orifice area in respective mitral valvular segments, ANT = anterior (grey), MID = middle (white), POST = posterior (checkered) at **A**: early systole (earlyS); **B**: midsystole (midS) and **C**: end-systole (endS), # = to facilitate data comparison data was zeroed at baseline EndS assuming minimum orifice opening under baseline conditions at that timepoint (see METHODS for details), * =p<0.05 vs baseline, ** =p<0.01 vs baseline, *** =p<0.001 vs baseline, data are group mean ±SEM

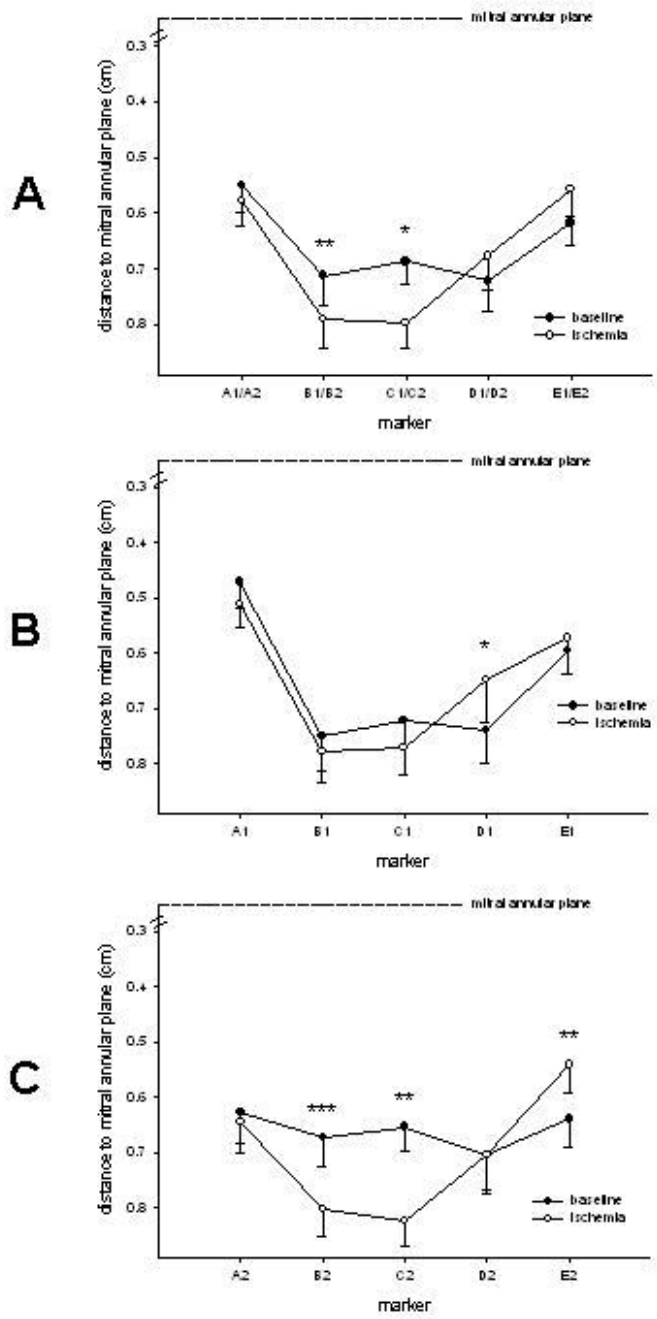

Fig 5.

A: Tenting height of different coaptation regions defined as the perpendicular distance from the midpoint of the two paired leaflet edge markers (A_1-A_2, B_1-B_2, C_1-C_2, D_1-D_2, E_1-E_2) to a best-fit plane containing the annular markers, **B**: Distances of anterior (A_1-E_1) mitral leaflet markers to the mitral annular plane; **C**: Distances of posterior(A_2-E_2) mitral leaflet markers to the mitral annular plane, *=p<0.05 vs baseline, **=p<0.01 vs baseline, ***=p<0.001 vs baseline, data are group mean ±SEM

TABLE 1

Hemodynamics

	Baseline	Ischemia
MR	0.5±0.3	2.3±0.7**
HR (min^{-1})	97±14	90±15
dP/dt_{max} (mmHg/s)	1950±600	1120±290**
LVEDP (mmHg)	18±3	25±5**
LVP_{EarlyS} (mmHg)	105±8.5	79.2±9.9***
LVP_{MidS} (mmHg)	92.5±34.7	69.3±24.4***
LVP_{EndS} (mmHg)	88.0±14.5 #§	61.0±10.3, ***#§

Group mean ±SD, MR=mitral regurgitation, HR= heart rate, LVP= left ventricular pressure, EarlyS= early systole, EndS= end- systole

*=p<0.05 vs baseline

**=p<0.01 vs baseline

***=p<0.001 vs baseline, using paired t-test,

#P<0.01 vs. EarlyS

§P<0.01 vs. MidS, using one-way repeated measures ANOVA with the Holm-Sidak post hoc test.

TABLE 2

Annular dimensions

	EarlyS		MidS		EndS	
	Baseline	**Ischemia**	**Baseline**	**Ischemia**	**Baseline**	**Ischemia**
MAA (cm^2)	7.86±2.62	9.78±4.40**	7.65±2.50	9.58±4.03**	7.63±2.64	9.85±4.08**
C-C (cm)	3.91±0.64	4.14±0.73***	3.84±0.67	4.09±0.69**	3.70±0.66	3.99±0.67***
S-L_{ANT} (cm)	1.92±0.46	2.15±0.69**	1.89±0.42	2.11±0.62**	1.86±0.37	2.11±0.55**
S-L_{MID} (cm)	2.78±0.79	3.26±1.14**	2.74±0.75	3.23±1.04***	2.67±0.76	3.20±1.03***
S-L_{POST} (cm)	2.63±0.56	3.04±0.87**	2.58±0.51	3.03±0.81**	2.50±0.54	2.99±0.80***

Group mean ±SD

MAA= mitral annular area, C-C = commissure-commissure diameter, S-L_{ANT}, S-L_{MID} and S-L_{POST} represent mitral annular anterior, mid and posterior septal-lateral diameters (see METHODS), EarlyS= early systole, MidS= mid-systole, EndS= end-systole (see METHODS for definition of timepoints)

* =p<0.05 vs baseline

** =p<0.01 vs baseline

*** =p<0.001 vs baseline

TABLE 3

Tethering lengths

	EarlyS		MidS		EndS	
	Baseline	**Ischemia**	**Baseline**	**Ischemia**	**Baseline**	**Ischemia**
- anterior PM (cm)	3.57±0.17	3.60±0.26	3.54±0.18	3.54±0.25	3.47±0.18	3.53±0.25
- posterior PM (cm)	3.88±0.30	4.00±0.29	3.85±0.31	3.98±0.33*	3.78±0.32	3.99±0.29**

Group mean±SD

PM=papillary muscle, EarlyS= early systole, MidS= mid-systole, EndS= end-systole (see METHODS for definition of timepoints)

* =p<0.05 vs baseline

** =p<0.01 vs baseline